Magnetic Properties of the Iron Arsenate Phase $Fe_2As_4O_{12}$. Short-Range versus Long-Range Order

A. M. Nakua and J. E. Greedan*

Chemistry Department and Institute for Materials Research, McMaster University, Hamilton, ON, Canada L8S 4M1

Received October 26, 1994[⊗]

A novel route for the preparation of $Fe_2As_4O_{12}$ is reported. This oxide crystallizes in the space group $P6_3$ with the unit cell dimensions $a = 14.743(7)$ Å and $c = 7.638(1)$ Å, with $Z = 6$. The main structural feature of this material is the presence of $Fe_2O_9^{12-}$ dimers which are connected with each other in a 3-D network via AsO_4^{3-} tetrahedra. Susceptibility data were measured down to 5 K. The susceptibility attains a maximum at about 50 K. Although the crystal structure favors dimer-like short-range ordering, long-range order dominates in this material and the dimer-like correlations are extremely weak or even absent. The data between 80 and 300 K were fitted to the Curie–Weiss law with an effective moment of 5.75(7) μ_B and Weiss constant equal to −95 K. The magnetically ordered state was studied by low-temperature neutron diffraction. The magnetic reflections were indexed on the chemical cell with the propagation vector $\mathbf{k} = (000)$, and the moments were found to lie normal to the c axis. The Néel temperature is 40 K.

Introduction

In the course of the preparation of other members of the transition metal arsenate series, AAs_2O_6, with the lead antimonate structure, the preparation of iron arsenate, $FeAs_2O_6$, was attempted. This was thought to be possible because the ionic radius ratio of Fe^{2+}/As^{5+} falls within the limits of the field of stability of the lead antimonate structure as suggested by Hill.[1]

An off-white reaction product was obtained which had a powder diffraction pattern which was strikingly different from that observed for the AAs_2O_6 arsenates as shown in Figure 1. Instead, the product was found to be the previously reported phase $Fe_2As_4O_{12}$, which was prepared first by d'Yvoire via the thermal decomposition of $Fe(AsO_3)_3$.[2]

Experimental Section

Since stoichiometric FeO does not exist, the synthesis was carried out by reacting a mixture of Fe powder (Alfa) and iron oxide Fe_2O_3 (Baker, 99.3%) with As_2O_5 (AESAR, 99.99%). The drying and evacuation procedures were outlined previously.[3] An off-white powder was obtained after this mixture was heated at 750 °C for 1 week in a sealed quartz tube.

The X-ray powder pattern of this product was obtained from a Nicolet-I2 diffractometer and a Guinier-Hägg camera (IRDAB XDC700) with Cu $K\alpha_1$ radiation. The Guinier films were read by a computer-controlled, automated LS-20 type line scanner (KEJ Instruments, Töby, Sweden).

Single crystals of this material were also prepared. This was done by loading 1 g of $Fe_2As_4O_{12}$ powder in a quartz tube with the dimensions 100 mm × 12 mm × 1 mm thickness. The sample tube was evacuated to 10^{-2} Torr, $^1/_2$ atm of Cl_2 gas was then introduced, and the tube was sealed off. The tube was soaked at 900 °C for 10 h and slowly cooled at a rate of 5 °C/h to 400 °C. The subsequent cooling to room temperature was done at a much higher rate. Large aggregates of white, transparent single crystals were obtained. Elemental analysis was done on one of these aggregates by using EDAX to rule out the presence of any chlorine in the sample. A small sample was used to measure the X-ray pattern in the Guinier camera. A pattern identical to that of the polycrystalline $Fe_2As_4O_{12}$ was observed.

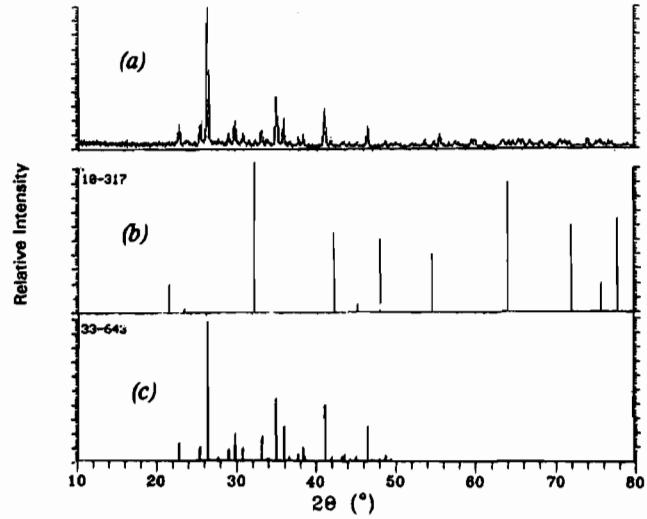

Figure 1. Powder X-ray diffraction for $Fe_2As_4O_{12}$: (a) observed intensity data for the product of reaction; (b) diffraction pattern for $CoAs_2O_6$; (c) diffraction pattern for $Fe_2As_4O_{12}$. (b) and (c) were obtained from the JCPDS data base.

Low-temperature neutron data were collected at the McMaster Nuclear Reactor, MNR, with 1.39-Å neutrons. The detector was a three-tube position sensitive detector which has been described previously.[4] The sample holder was an aluminum can with helium exchange gas which was sealed with an indium gasket.

Magnetic susceptibility data were collected on a Quantum Design SQUID magnetometer using a pressed polycrystalline pellet. The magnetometer was calibrated with high-purity palladium.

Results and Discussion

This compound is best formulated as $Fe^{3+}{}_2As^{3+}As^{5+}{}_3O_{12}$. Evidently, Fe^{2+} and As^{5+} are thermodynamically incompatible in oxide crystals of this type. This argument is supported by the fact that all of the iron arsenates reported in the JCPDS data base were found to contain iron in the trivalent state only.

$Fe_2As_4O_{12}$ crystallizes in the hexagonal space group $P6_3$, and the unit cell dimensions were $a = 14.743(7)$ Å and $c =$

* To whom correspondence should be addressed.
⊗ Abstract published in *Advance ACS Abstracts,* February 15, 1995.
(1) Hill, R. *J. Solid State Chem.* **1987**, *71*, 12.
(2) d'Yvoire, F. *Bull. Soc. Chim. Fr.* **1974**, 1215.
(3) Nakua, A. M.; Greedan, J. E. *J. Solid State Chem.*, in press.
(4) Reimers, J. N.; Greedan, J. E.; Sato, E. *J. Solid State Chem.* **1988**, *72*, 390.

0020-1669/95/1334-1373$09.00/0

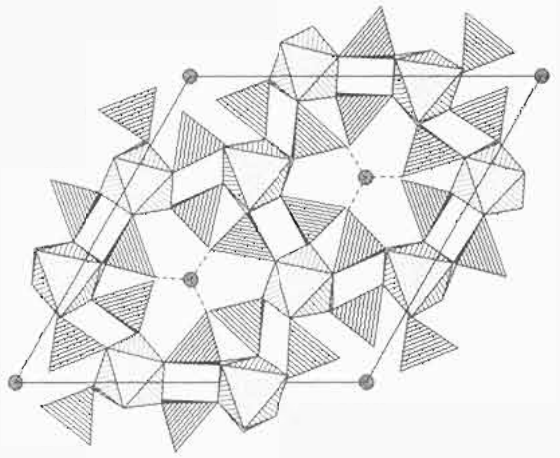

Figure 2. The (001) projection of the $Fe_2As_4O_{12}$ structure. AsO_4 tetrahedra are connected by an $As^{3+}O_3$ pyramid, shown as dashed lines, and connected to the $Fe_2O_9^{12-}$ dimers, dotted polyhedra.

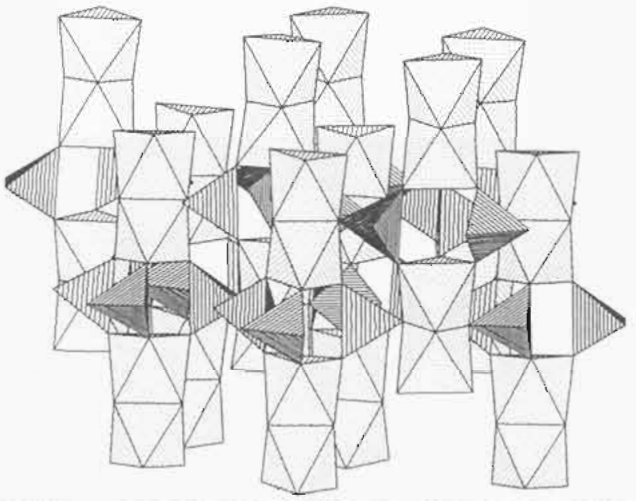

Figure 3. Structural framework of $Fe_2As_4O_{12}$, which consists of two iron octahedra sharing faces and forming the $Fe_2O_9^{12-}$ dimers which are connected by AsO_4 tetrahedra to form the 3-dimensional network.

7.638(1) Å, and $Z = 6$, which are in good agreement with those reported by d'Yvoire.[2]

d'Yvoire *et al.* solved the crystal structure of this compound using single-crystal X-ray diffraction.[5] Therefore, our objective in the present study was primarily to study the magnetic properties of this compound and ultimately to correlate, if possible, our findings with the crystal structure.

$Fe_2As_4O_{12}$ has a very complicated and remarkable 3-dimensional framework as illustrated by the (001) projection in Figure 2. As^{3+} is coordinated to three oxygen atoms forming a central pyramid, AsO_3^{3-}, which is bonded to three tetrahedral groups AsO_4^{3-} via the O atoms. The most interesting feature of this structure is the presence of discrete face-sharing $Fe_2O_9^{12-}$ dimers which can be viewed more clearly in Figure 3. The Fe ion is in octahedral coordination with an average Fe−O distance of 2.012 Å. The Fe−O−Fe angles average to 91.5(4)°, and the Fe--Fe separation is 3.03 Å. The dimers are in turn interconnected by discrete arsenate ions. This structure, therefore, presents the possibility of both a dimer-confined short-range order and a long-range magnetically ordered state. Both of these possibilities were thoroughly investigated by analyzing magnetic susceptibility and low-temperature neutron diffraction data.

(1) Magnetic Susceptibility. Magnetic susceptibility was measured on a polycrystalline sample in the temperature range

(5) d'Yvoire, F.; Hug Nguyen, D. *Acta Crystallogr.* **1979**, *B35*, 1751.

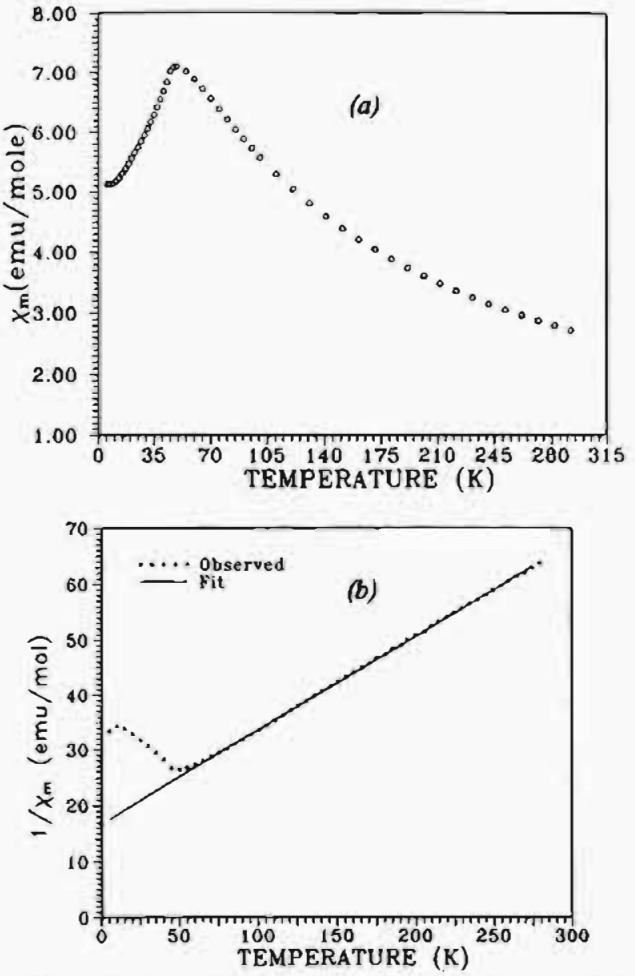

Figure 4. Magnetic susceptibility of $Fe_2As_4O_{12}$: (a) magnetic susceptibility versus temperature; (b) inverse of the magnetic susceptibility versus temperature. Circles represent the observed data, and solid line denotes the prediction of the Curie−Weiss fit.

5−300 K. The susceptibility attains a maximum of 7.65×10^{-2} emu/mol at approximately 50 K, below which a sharp decrease was observed, suggesting a transition to long-range order as can be seen in Figure 4.

After diamagnetic corrections, the data in the range 80−300 K were fitted to a Curie−Weiss law, with an effective magnetic moment of 5.75 μ_B, in good agreement with the expected value for the high-spin Fe^{3+}, 5.92 μ_B, and a Weiss constant equal to −95 K. A plot of the inverse susceptibility data and the predictions of the Curie−Weiss law are shown in Figure 4. Remarkably, there is no noticeable deviation from the Curie−Weiss law which would be expected if significant short-range correlations were present. It was expected that the magnetic susceptibility would be dominated by the antiferromagnetic exchange within the $Fe_2O_9^{12-}$ dimer units.

The absence of any significant short-range correlations in the susceptibility data is likely to be due to two reasons. First, the angle Fe−O−Fe is sharply different from 180°, which will cause the magnitude of the interaction constant to be very small and thus will result in a weaker intradimer interaction. A correlation between the exchange constant and the angle M−O−M has been observed in many systems. The classical example is the dihydroxy-bridged copper(II) dimers in which the exchange constant decreases as the Cu−O−Cu angle deviates from 180° until the bond angle reaches 97.6°, after which the ferromagnetic coupling dominates over the antiferromagnetic coupling.[6] In fact, there is a linear relationship between J and Θ in a series of dihydroxy-bridged copper(II) dimers. Magnetism in oxo-

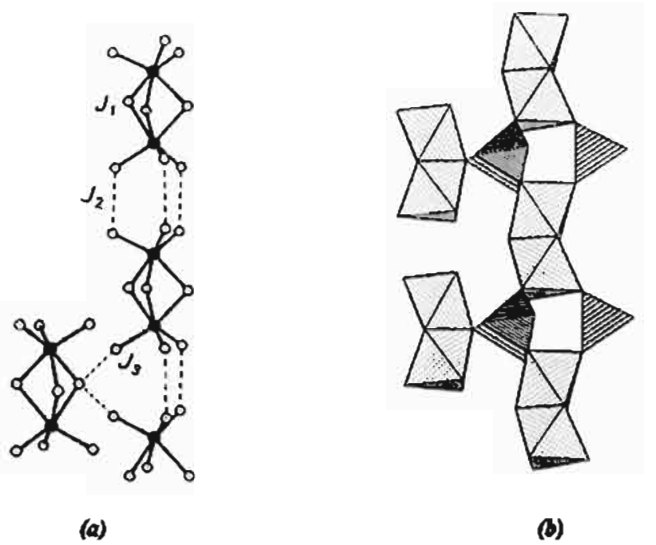

Figure 5. Possible exchange pathways in the $Fe_2As_4O_{12}$ structure. (a) J_1 is the intradimer interaction; J_2 and J_3 are the interdimer interactions. (b) Polyhedral presentation of the portion of the structure: dotted octahedra represent the $Fe_2O_9^{12-}$ dimers, and tetrahedra are AsO_4.

bridged diiron dimers has been reviewed by Kutz[7] and Hotzelmann *et al.*[8] Contrary to the case of Cu-based dimers, there was a general lack of linear relationships between J values and structural parameters which was attributed to a relatively complex interplay of competing orbital pathways for spin coupling and a sensitivity to multiple structural variables, *e.g.* bond length, bond angle, and spin distribution. What is clear is that the antiferromagnetic coupling diminishes as the Fe−O−Fe angle becomes more acute; for instance, the exchange constant, J/k, in $[Fe(salen)(OH)]_2$ is −14.4 K (−10 cm^{-1}), with an Fe−O−Fe angle 102°, and −132 K for $Fe(salen)_2O$, where the Fe−O−Fe angle is 145° (salen = *N,N'*-ethylenebis(salicylamide)).[9,10] The spin coupling in high-spin d^5 Fe^{3+} dimers is almost invariably antiferromagnetic in nature for Fe−O−Fe angles between 180 and 110°. Yet it was reported by Snyder *et al.* and Mikuriya *et al.* that dimers with Fe−O−Fe bridge angles below 97° actually show very weak, J = 1−2 cm^{-1} (1.44−2.88 K), ferromagnetic intradimer exchange coupling.[11,12] As the Fe−O−Fe angle for $Fe_2As_4O_{12}$ falls into this range, it is possible to assign a weak ferromagnetic intradimer coupling here as well.

The second factor that comes into play is that other superexchange pathways become important. In addition, these interdimer interactions outnumber the intradimer exchange interactions and hence their sum can overwhelm the intradimer interaction. The possible interdimer exchange pathways in this compound are illustrated pictorially in Figure 5, in which the $Fe_2O_9^{12-}$ dimer is connected to two dimers along the ⟨001⟩ direction via three AsO_4 tetrahedra, exchange pathway J_2, and to another three dimers in the basal plane also via AsO_4 tetrahedra, pathway J_3.

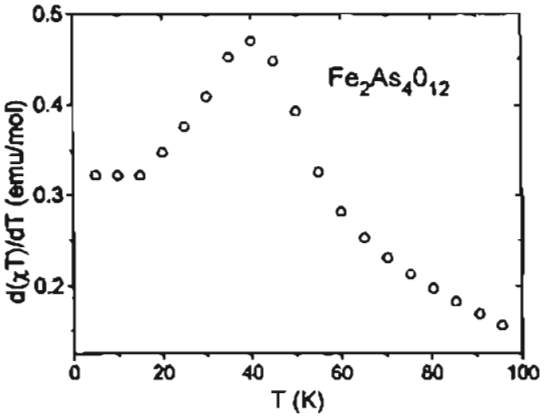

Figure 6. Fisher's specific heat for $Fe_2As_4O_{12}$.

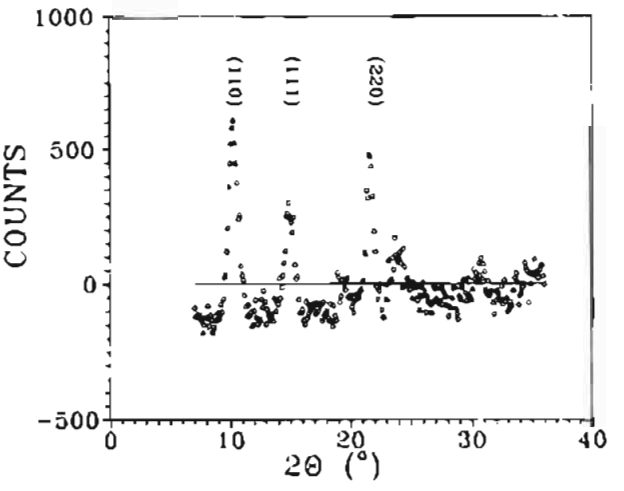

Figure 7. Difference plot of the neutron diffraction profiles of $Fe_2As_4O_{12}$ at 10 and 57 K.

It is plausible to analyze the susceptibility data of Figure 4 by the method suggested by Fisher to obtain an approximation to the magnetic specific heat.[13] A plot of $d(\chi T)/dT$, Figure 6, shows a sharp spike at 40 K which likely *is* due to a long range-order transition. The temperature at which this spike occurs is a more accurate estimate of the transition temperature than that which corresponds to the maximum in the susceptibility data.

(2) Long-Range Order. The sharp decrease in the magnetic susceptibility data below 50 K then suggests the presence of magnetic long-range order in this system. To investigate this further, low-temperature neutron scattering data were collected on the powder sample at various temperatures. The scattering pattern of $Fe_2As_4O_{12}$ at 9 K contains a number of very intense magnetic reflections. These reflections could be more clearly identified in the difference plot as in Figure 7, in which the most intense magnetic reflections have 2θ values of 10.30, 15.02, and 21.5°. It is possible to index these magnetic reflections on the chemical cell as (110), (111), and (220), respectively, giving a propagation vector of $\mathbf{k}$ = (000).

Figure 8 summarizes the temperature dependence of the intensity of the magnetic reflections which *decrease* rapidly near 50 K, indicating that they are magnetic in origin. Since the intensity of the magnetic scattering at zero-field is proportional to the square of the spontaneous magnetization, the temperature dependence of the magnetization can be used as an accurate method to determine the transition temperature. Thus, the variation of the magnetization of the (110) reflection as a function of temperature suggests that the T_c is about 40 K, as

(6) Hatfield, W. In *Magneto-Structural Correlations in Exchange Coupled Systems*; Willett, R., *et al.*, Eds.; D. Reidel Publishing Co.: Dordrecht, The Netherlands, 1985; p 555.
(7) Kutz, D. M., Jr. *Chem. Rev.* **1990**, *90*, 585.
(8) Hotzelmann, R.; Wieghardt, K.; Flörke, U.; Haupt, H.; Weatherburn, D. C.; Bonvoisin, J.; Blondin, G.; Girerd, J. J. *Am. Chem. Soc.* **1992**, *114*, 1681.
(9) Borer, L.; Thalken, L.; Ceccarelli, C.; Glick, M. J.; Zhang, J. H.; Reiff, W. M. *Inorg. Chem.* **1983**, *22*, 1719.
(10) Mukherjee, R. N.; Stack, T. D. P.; Holm, R. H. *J. Am. Chem. Soc.* **1988**, *110*, 1850.
(11) Snyder, B. S.; Patterson, G. S.; Abrahamson, A. J.; Holm, R. H. *J. Am. Chem. Soc.* **1989**, *111*, 5214.
(12) Mikuriya, M.; Kakuta, Y.; Kawano, K.; Tokii, T. *Chem. Lett. (Jpn.)* **1991**, 2031.
(13) Fisher, M. *Philos. Mag.* **1962**, *17*, 1731.

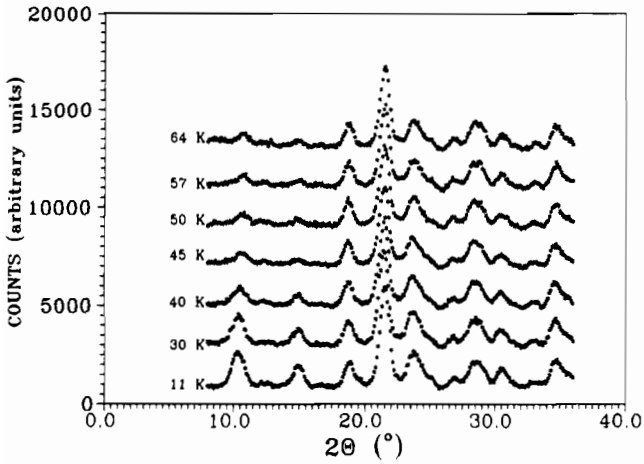

Figure 8. Variation of the neutron scattering intensity for $Fe_2As_4O_{12}$ as a function of temperature.

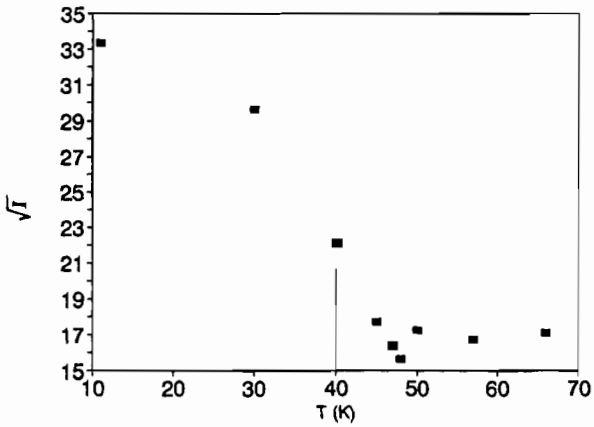

Figure 9. Temperature dependence of the square root of the intensity of the (110) reflection for $Fe_2As_4O_{12}$. The value of T_N obtained from Fisher's method is also indicated by the vertical bar at 40 K.

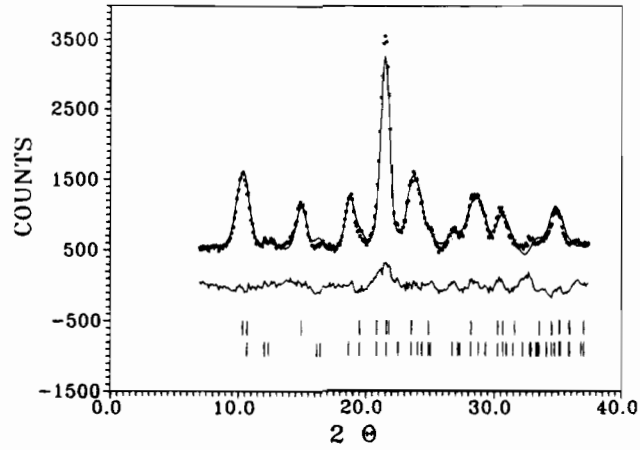

Figure 10. Rietveld refinement pattern of the low-temperature neutron diffraction data for $Fe_2As_4O_{12}$. The upper set of bars indicates the magnetic Bragg peaks, and the lower set corresponds to the nuclear Bragg peaks.

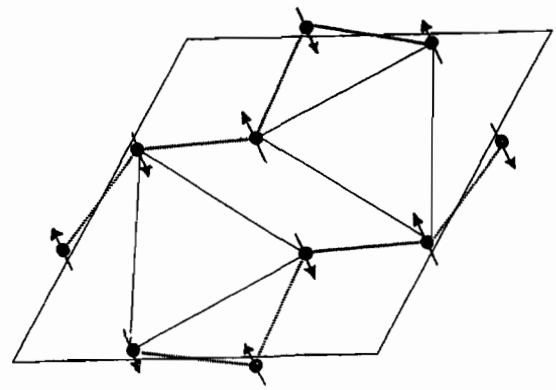

Figure 11. Spin arrangement in the magnetic sublattice for $Fe_2As_4O_{12}$ in one puckered plane showing the interactions in the plane. Another layer of moments resides underneath this layer and couples antiferromagnetically with the moments in the plane shown.

illustrated in Figure 9, which is in good agreement with the T_c obtained from the Fisher's specific heat analysis. The choice of the (110) reflection for these calculations is due to the fact that it is the most intense magnetic reflection of this material. As for the nuclear contribution to the intensity of this reflection, it is not substantial in comparison with the magnetic part of the intensity and these two terms are additive in the case of unpolarized neutrons so it is believed not to affect the results.

In an effort to determine the magnetic structure *for* this material, we carried out Rietveld profile refinement of the low-temperature neutron data using the RIETAN program.[14] This program is capable of modelling neutron scattering from magnetic structures with collinear arrangements. As an initial model, it was assumed that spins in the dimers are coupled antiparallel and that the spins in the same puckered layers are coupled parallel. This model gave an unsatisfactory fit to the data. After some trial and error, another model was found which gave a more satisfactory fit, and this is represented in Figure 11. In fact, Figure 11 depicts one slightly puckered layer; a second such layer with antiparallel spins directly above those shown is not included. Note that the spins lie in the hexagonal plane. The refinement was carried out in space group $P3$, and only the Fe moment, its orientation, and its overall temperature factor were varied due to the relatively large number of positional parameters involved. The agreement indices are R_{wp} = 0.081, R_p = 0.065, and R_{exp} = 0.033, where these are defined in the conventional manner.[15] The Fe^{3+} moment refines to 5.1(4) μ_B, which is slightly large but the error is also large. This may reflect the use of an overall temperature factor in the refinement. The spin arrangement found is consistent with J_2, $J_3 < 0$ and $|J_2| \approx |J_3|$. This is reasonable as both J's correspond to similar exchange pathways, Fe−O−As−O−Fe. The observed magnetic structure does not preclude a finite $J_1 < 0$, but the absence of dimer-like short-range order in the magnetic susceptibility indicates that J_1 is small relative to J_2 and J_3.

The fact that the relation between the magnetic behavior and the crystal structure is not always straightforward is well illustrated by this example. It is interesting to investigate the effect the change of the magnetic ion will have on the overall magnetic behavior of this structure, for example by studying the isostructural compound, $Cr_2As_4O_{12}$. Initial magnetic susceptibility data reported by D'Yvoire suggest the presence of stronger antiferromagnetic intradimer correlations in this material.[2]

Acknowledgment. We thank Dr. C. V. Stager for use of the SQUID magnetometer. This work was supported by the Natural Science and Engineering Research Council of Canada. A.M.N. acknowledges financial support from the Secretariat for Scientific Research of Libya.

IC941235C

(14) Izumi, F. *Rietan-Rietveld Analysis Systems*; National Institute for Research in Inorganic Materials: Ibaraki, Japan, 1985; *Nippon Kessho Gakkai Shi* **1985**, *27*, 23.

(15) Young, R. *The Rietveld Method*; Young, R., Ed.; Oxford University Press: Oxford, U.K., 1993; Chapter 1.